2E5-2

Proceedings of Symposium on Ultrasonic Electronics, Vol. 33 (2012) pp. 143-144
13-15 November, 2012

Three-dimensional Interactive Detection and Localization of Small Metastatic Foci in Human Lymph Nodes Using High-frequency Quantitative Ultrasound

Jonathan Mamou[‡,1], Emi Saegusa-Beecroft[2], Alain Coron[3,4], Michael L. Oelze[5], Masaki Hata[2], Junji Machi[2], Eugene Yanagihara[2], Pascal Laugier[3,4], Tadashi Yamaguchi[6] and Ernest J. Feleppa[1]

([1]F. L. Lizzi Center for Biomedical Engineering, Riverside Research Institute, New York, NY, [2]Univ. of Hawaii and Kuakini Medical Center, Honolulu, HI, [3]UPMC Univ. of Paris 06, UMR 7623, LIP, Paris, F-75005 France, [4]CNRS, UMR7623 Laboratoire d'Imagerie Paramétrique, Paris, F-75006 France, [5]Dept. of Electrical and Computer Engineering, Univ. of Illinois at Urbana-Champaign, Urbana, IL, [6]CFME, Chiba Univ., Chiba, Japan)

1. Introduction

Detection of small metastatic foci in dissected human lymph nodes of cancer patients is critically important for treatment. However, current state-of-the art histopathology procedures are too labor intensive to allow evaluating all dissected nodes in their entirety. They microscopically examine only thin sections obtained from the central plane of each dissected node, and small but clinically important metastatic foci can be overlooked leading to a false-negative diagnosis. In this study, we investigate the use of novel three-dimensional (3D) quantitative ultrasound (QUS) methods to evaluate dissected nodes in their entirety. These QUS methods rely on frameworks developed during the past three decades to obtain QUS estimates that quantify tissue properties [1, 2]. Our hypothesis is that QUS methods using high-frequency ultrasound (HFU, >20 MHz) have the ability to detect small metastatic foci because these methods permit quantifying tissue properties at the microscopic level with fine spatial resolution (<100 μm). In recent studies, we have investigated 13 QUS estimates derived from the quantification of envelope signal statistics and spectra of backscattered radio-frequency (RF) signals. An interactive graphical user interface (GUI) was developed to permit virtual 3D exploration of lymph nodes by displaying orthogonal cross-sectional views. In addition, *a posteriori* cancer probabilities were estimated at each voxel based on the QUS estimates and displayed using the GUI.

2. Methods

Patients who were scheduled for surgery to treat proven gastric, colorectal, or breast cancers were recruited for the study at the Kuakini Medical Center (KMC) in Honolulu, HI. According to standard practice, regional lymph nodes were dissected surgically and excised tissue specimens were sent to the KMC pathology laboratory where individual lymph nodes were prepared for ultrasound scanning and histology.

For ultrasound scanning, individual lymph nodes were immersed in an isotonic saline (0.9% sodium chloride) bath at room temperature and were ultrasonically scanned in 3D using a single-element transducer (PI30, Olympus NDT, Waltham, MA) and custom HFU scanning system. The transducer had an aperture of 6.1 mm, an F-number of 2, a center frequency of 25.6 MHz, and a -6 dB fractional bandwidth of 67%. The backscattered ultrasound RF signals were digitized at 400 MS/s with 8-bit accuracy. Adjacent planes and RF lines were 25 μm apart to cover the entire node in 3D with sufficient spatial sampling.

To guarantee the accurate detection of small metastatic foci, the lymph node underwent rigorous non-standard histology processing following ultrasound scanning. Briefly, the node was inked to recover orientation, cut in half, embedded in a cassette, fixed, sectioned at 50-μm intervals, and then stained with H&E. Digital photomicrographs of the stained slides were obtained with a slide scanner (NanoZoomer, Hamamatsu, Japan) with a pixel resolution of 0.46 μm. Metastatic regions were then highlighted in each digital image using custom software.

The raw RF data were processed to yield the 13 QUS estimates. First, the 3D RF volume of data was separated into overlapping 3D cylindrical regions of interest (ROIs) of 1-mm diameter and 1-mm length. Second, the normalized power spectrum of each ROI was estimated to obtain four QUS estimates using two independent ultrasound scattering models [3]. Third, the probability-density function (PDF) of the envelope of the ROI was computed to obtain the remaining 9 QUS estimates by fitting two different envelope-statistics models and by quantifying the difference between the PDF of the ROI and the Rayleigh PDF [3,4]. This

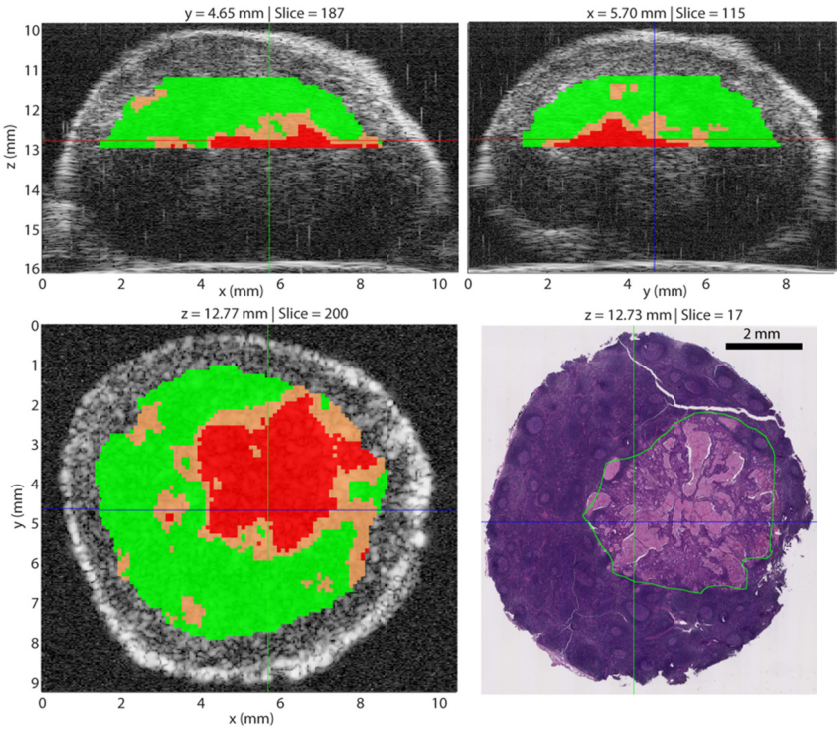

Fig. 1 Screen capture from the GUI showing a partially-metastatic lymph node from a colorectal-cancer patient. Three conventional B-mode images are shown augmented with color-coded cancer probability. Red indicates cancer probability greater than 75%, green highlight indicates cancer probability smaller than 25%, and orange indicates values between 25% and 75%. The bottom-right panel displays the co-registered histology with cancerous regions outlined in green. Comparison of the two bottom panels shows that the QUS methods reliably detect the metastatic foci.

elegant method used to quantify the divergence from a Rayleigh-distributed ROI was adapted from a previous study that successfully quantified liver fibrosis [4]. The 13 QUS estimates were linearly combined using Fisher linear-discriminant analysis to maximize classification performance and to obtain a scalar variable (i.e., the discriminant score) for each ROI of each lymph node. *A posteriori* cancer probabilities were computed based on these discriminant scores. Classification performance was evaluated by computing an ROC curve and estimating the area under the curve (AUC). Finally, the GUI was developed to provide interactive display of the three orthogonal cross-sections of grayscale B-mode data or of B-mode data overlaid with color-encoded cancer-probability estimates.

3. Results

More than 250 lymph nodes from more than 110 patients were processed. Data obtained from lymph nodes entirely filled or entirely devoid of metastatic tissue were used to train and test the classifiers and, because of their structural differences, results of gastric, colorectal, and breast cancer nodes were separated and three distinct classifiers were obtained. Classification of the gastric-, colorectal-, and breast-cancer nodes gave AUC values of 0.95, 0.96, and 0.85, respectively.

Figure 1 shows a screen capture of one of the GUI modes. A partially-metastatic lymph node obtained from a colorectal-cancer patient is illustrated. The GUI displays three orthogonal cross-sectional conventional B-mode images with color-coded cancer-probability ranges overlaid; red indicates probability of 75% or more, orange indicates probability between 75% and 25%, and green indicates probability of 25% or less. Finally, the bottom-right panel displays the co-registered histology photomicrograph corresponding to the bottom-left QUS image. Metastatic regions are outlined in green in the histology image. Excellent concurrence is evident between the high-probability region in the lower-left QUS image and the demarcated cancerous region in the corresponding lower-right histology image.

4. Conclusions

These studies indicate that the QUS methods applied in 3D to dissected lymph nodes can detect and localize metastatic regions within lymph nodes with satisfactory specificity and sensitivity. Furthermore, the interactive GUI permits exploring results in 3D and can serve as a model for development of a new pathology device to guide pathologists towards suspicious regions quickly and reliably. This device could significantly reduce the rate of false-negative determinations allowed by current standard histology procedures, which examine only the central plane of each lymph node.

Acknowledgments

This research was supported in part by NIH grant CA100183, Ernest Feleppa, Principal Investigator.

References

1. F. L. Lizzi, M. Greenebaum, E. J. Feleppa, M. Elbaum and D. J. Coleman: J. Acoust. Soc. Am. **73** (1983) 1366.
2. M.F. Insana, R. F. Wagner, D. G. Brown, T. J. Hall: J Acoust Soc Am. **87**(1990) 179
3. J .Mamou, A. Coron, M. L. Oelze, E. Saegusa-Beecroft, M. Hata, P. Lee, J. Machi, E. Yanagihara, P. Laugier, and E. J. Feleppa Ultrasound Med Biol. 37 (2011) 345.
4. T. Yamaguchi and H. Hachiya, J. Med. Ultrasonics **37** (2010), **1**55.